DOI:10.2298/CSIS120531014F

Biomechanical Modeling of Knee for Specific Patients with Chronic Anterior Cruciate Ligament Injury

Nenad Filipović[1,2], Velibor Isailovic[1,2], Dalibor Nikolić[1,2], Aleksandar Peulić[3], Nikola Mijailović[1,2], Suzana Petrović[1], Saša Cuković[1], Radun Vulović[1,2], Aleksandar Matić[3], Nebojša Zdravković[3], Goran Devedžić[1] and Branko Ristić[3]

[1] Faculty of Engineering, University of Kragujevac, Sestre Janjica 6,
34000 Kragujevac, Serbia
fica@kg.ac.rs
[2] Bioengineering Research and Development Center, Prvoslava Stojanovica 6,
34000 Kragujevac, Serbia
bioirc@kg.ac.rs
[3]Technical Faculty,
32000 Cacak, Serbia
[4] Medical Faculty, University of Kragujevac, Svetozara Markovica 69,
34000 Kragujevac, Serbia
branko.ristic@gmail.com

Abstract. In this study we modeled a patient specific 3D knee after anterior cruicate ligament (ACL) reconstruction. The purpose of the ACL reconstruction is to achieve stability in the entire range of motion of the knee and the establishment of the normal gait pattern. We present a new reconstruction technique that generates patient-specific 3D knee models from patient's magnetic resonant images (MRIs). The motion of the ACL reconstruction patients is measured by OptiTrack system with six infrared cameras. Finite element model of bones, cartilage and meniscus is used for determination stress and strain distribution at different body postures during gait analysis. It was observed that the maximum effective von Mises stress distribution up to 8 MPa occurred during 30% of the gait cycle on the meniscus. The biomechanical model of the knee joint during gait analysis can provide insight into the underlying mechanisms of knee function after ACL reconstruction.

Keywords: ACL reconstruction, knee motion, gait analysis, biomechanical finite element modeling.

1. Introduction

There is always a question what are dynamic loading conditions to which cartilage is exposed during daily activity. It is fundamental for diagnosing and treating joint disease, since dynamic loading affects the movement of tissue growth factors [1].

Interaction between several factors (anatomical, functional and biological) has influence on cartilage degeneration. Determining cartilage progression rate is based on defining abnormal loadings during gait cycle which contribute to cartilage wear.

Many researchers analyzed biomechanical models of the knee joint based on the finite element method. These models provide significant insight into the stress and strain distribution and contact kinematics at the knee joint [2], [3], [4], [5], [6] and have been used to investigate the effect of ligament injury [7], [8]. In these studies the knee joint was generally subjected to axial loads with the knee flexion angle fixed and subject-specific data were not used to define the joint geometry and loading conditions. To address these shortcomings, here, we propose a construction of subject-specific biomechanical model of the human knee joint by combining magnetic resonance imaging (MRI) of the knee joint, motion analysis measured with camera system and finite element analysis of subject-specific 3D knee models.

2. Related Work

Normal knee functions lie in complex relationship of the movement and stability. Knowing knee kinematics is of great importance for getting relevant knee functions information which can be used for improving treatment of the knee pathology.

Clinical and functional indicators of the surgery results of the anterior cruciate ligament show decrease of the tibial translation during gait activity in the postoperative period. Some studies show patients' ability to reduce tibial translation at the deficient knee although knee laxity is obvious. Reduction of the tibial translation is influenced by muscle activity. Primary task of the reconstruction surgery is to reduce translation of the tibia in the sagittal plane [9], [10], [11].

Tibial translation generally drives knee stability after anterior cruciate ligament reconstruction. The problem can still develop in spite of a decrease in excessive anteroposterior tibial translation after surgical procedure.

K. Manal et al. show that movement of the soft tissue of the lower limb could influence on the appearance of error during estimation of the tibial translation [12]. B. Gao et al. show that there exists significant change in the joint kinematics between deficient anterior cruciate ligament and healthy knee. After reconstructive surgery some differences corrected, but normal knee kinematics is not completely restored. In this study for measured

purposes we used method for gait analysis and optimization algorithm in order to reduce analysis errors caused by movement of the soft tissue [13].

According to the numerous studies during in vitro and in vivo experiments tibial translation along AP direction has been noticed in the case of the deficient anterior cruciate ligament knee, which confirms the findings in our study, shown at the Figure 3 [14], [15]. Maximal values of the tibial translation along ML, IS, and AP directions appear in the early stance phase. The ligament reconstruction surgery decreases tibial dislocation along all above mentioned directions.

The stability of the human knee joint is influenced by comprised elements such as ligaments, menisci and muscles. If deficient anterior cruciate ligament knee is not reconstructed, it indicates degenerative process on the cartilage [8], [9], [15].

In this paper we used a nonlinear porous finite element analysis for cartilage and meniscus and linear model for knee stability after anterior cruciate ligament reconstruction. It is very important to better understand cartilage and meniscus behavior to different loading condition. Many medical doctors found that the cartilage injury was most severe over the superficial zone of the posterior lateral tibia. It is impossible to measure injury in vivo patients even with today's state of the art for the image reconstruction methods. By comparing the computer simulation stress and strain cartilage and meniscus values we will be able to assess the severity of each patient's injury more accurately.

The paper is organized as following. We firstly present methods for experimental measurement, 3D image segmentation and reconstruction and finite element model of cartilage and meniscus. Then some results for coupled measurement and computational analysis are described. At the end some discussion and conclusion remarks are given.

3. Methods

3.1. Experimental measurements

Gait analysis was performed with nineteen adult men which are voluntarily participated in the experimental measurements. Subjects had a mean height of 183.33cm (S.D. 2.24), mean weight of 86kg (S.D. 3.48) and mean age of 29.89 years (S.D. 1.73). Subjects are recreational or professional sportsmen. Test analysis and surgery were performed at Clinical Centre Kragujevac, (Clinic for Orthopedics and Traumatology).

Kinematic data were collected with a three – dimensional (3D) motion analysis system (OptiTrack). This system consist of recording software ARENA and six infrared cameras (V100:R2) resolution 640x480 pixels with frame rate of 100 fps. Cameras were placed along a pathway. For defining

and processing kinematic data the global coordinate system was used because it is stationary, it does not depend on the subject and it is not influenced by marker's position. Global coordinate system was defined with z – axis coincidence with inferior - superior (IS) direction, x – axis coincidence with medial - lateral (ML) direction, and y – axis coincidence with anterior - posterior (AP) direction [8].

The study was performed in order to define kinematics data of the lower limb during performing gait activities in patients with deficient anterior cruciate ligament of the knee. Four passive reflective markers were placed at the anatomical landmarks of the lower extremity in order to minimize muscle activity. Landmarks were defined at the great trochanter region (GTR), at the femoral lateral epycondile (LEF), at the tuberosity of the tibia (TT), and in the region of the center of the ankle joint (CAJ) (Fig.1).

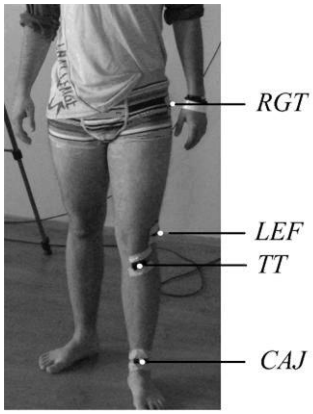

Fig. 1. The marker set used in the gait analysis experiment

Subjects performed normal walk at a self – selected speed along pathway about 5.00m. The day before surgery were recorded signals, first at the knee with deficient AC ligament, and then at the healthy knee. Every subject was asked to perform this task four times. Experiments are repeated after 15 days, and after 6 weeks. In this paper the results of the gait analysis after 6 weeks are shown.

Since subjects had deficient anterior cruciate ligament of the knee, during walking (Fig.2), in one moment (point TTi) the knee is stable, but in the next moment there is a tibial shift (point TTi+1).

According to above mentioned, tibial dislocation was defined by successive calculating the affine coordinates along IS, ML, and AP directions [9] with equations (1)-(3):

$$d_{TTAP} = (TTAP)_{i+1} - (TTAP)_i , \quad (1)$$

$$d_{TTML} = (TTML)_{i+1} - (TTML)_i , \quad (2)$$

$$d_{TTIS} = (TTIS)_{i+1} - (TTIS)_i \,. \tag{3}$$

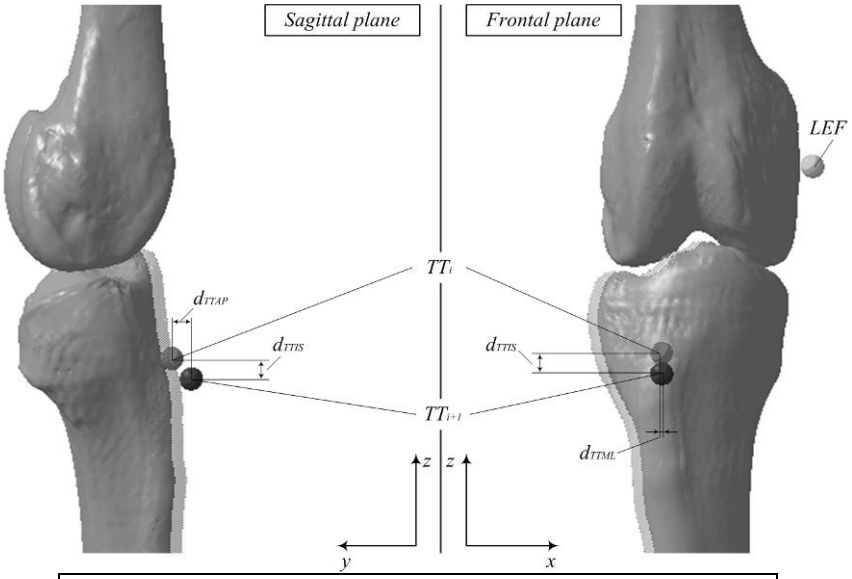

LEGEND:
LEF – lateral epycondil of the femur,
TTi – tuberosity of the tibia in i-th moment,
TTi+1 – tuberosity of the tibia in i+1-th moment,
dTTAP – tibial dislocation along AP direction,
dTTML – tibial dislocation along ML direction, and
dTTIS – tibial dislocation along IS direction.

Fig. 2. Tibial dislocation along ML, IS, and AP directions

Using obtained data point we apply eight order Fourier series approximation to estimated the curves of tibia dislocation for a specific patient (Fig.3).

The diagrams in Figure 3 indicate that tibial dislocations along ML and IS directions before and after surgery are very small, and they do not have big influence on the knee stability [9], [10]. Mean value of the tibial translation before surgery along ML direction is:0.656 mm (S.D. 0.512 mm), and along IS direction is 0.553 mm (S.D. 0.445 mm). It can be seen that values of the tibial translation along ML and IS direction decreased after surgery. Mean values of these translations along ML direction is 0.387 mm (S.D. 0.324 mm), and along IS direction is 0.122 mm (S.D. 0.099 mm).

AP translation has big influence on the knee stability at knees with deficient anterior cruciate ligaments. The fitted curves on Figure 3 which describe AP translation have high amplitudes [9], [10]. In swing phase of the gait cycle which correspond to 40% of the horizontal axis can be seen sharp

decline of the curve before surgery. Mean value of the AP translation before surgery is 4.543 mm (S.D. 3.658 mm). After ligament reconstruction, motion curve of the tibial translation has lower amplitudes and shows stability in swing phase. Mean value of the AP translation after surgery is 6.623 mm (S.D. 0.662 mm).

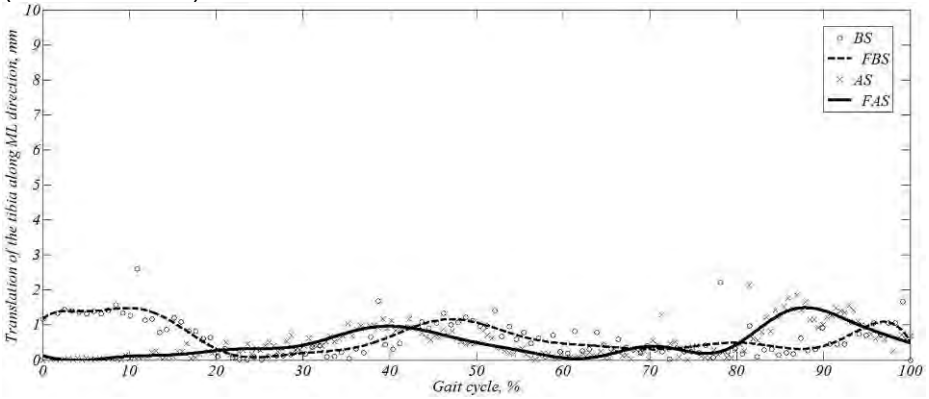

a)

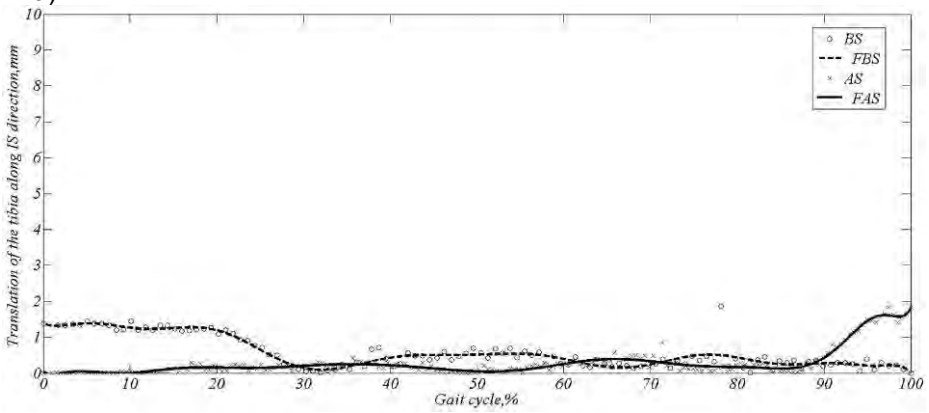

b)

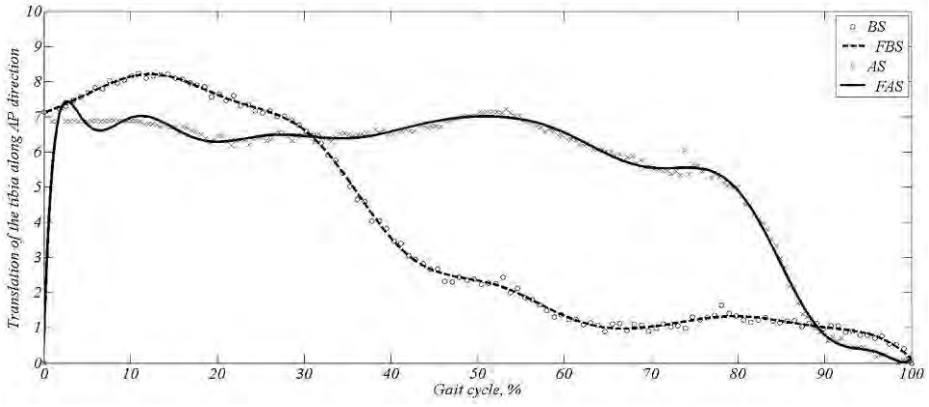

c)

LEGEND:
BS – Curve of the translation of the tibia before surgery, **FBS** – Fitted curve of the translation of the tibia before surgery, **AS** - Curve of the translation of the tibia after surgery, **FAS** – Fitted curve of the translation of the tibia after surgery.

Fig. 3. Translation of the tibia along: a) ML direction, b) IS direction, and c) AP direction

Student t – test was used for purpose of the statistical significance of the experimental results. It can be seen that there was significant difference in tibial translation along IS, ML, and AP directions in preoperational and post operational period for possible error $p< 0.01$ and for certainty of the $P>99\%$.

3.2. Computational method

We take geometry of the finite element model from MRI slices for a specific patient after surgery. Our in-house implementation includes an interface for users to adjust the position of the virtual cutting plane to better match with the MRI slices. A user can also make hand corrections on the knee contours after the automatic segmentation process finish. Four reflective markers at the anatomical landmarks of the lower extremity are detected on MRI 3D reconstruction object.

Figure 4 shows the interface of our knee segmentation system.

The algorithm for image segmentation and 3D object reconstruction from the MRI slices is following. Over all pixels a FE-mesh, initially uniform, is isotropically generated. We positioned the nodes of the FE-mesh at the centers of the existing voxels. This means that each FE overlaps 2x2 voxels in the 2D case or 2x2x2 voxels in the 3D case. The black circles represent nodes generated inside the object and the white circles denote nodes outside of the object. The nodes inside the object have a pixel or voxel value higher than the chosen threshold and the nodes outside the object have a value lower than the chosen threshold. Each FE node is assigned the grayscale value of the corresponding voxel. Note that the boundary between the black and white nodes is not smooth at this stage.

Because the FE-mesh is located on the surface boundary, some of its nodes (shown as the white circles) are on the outside of the object. Additionally, the grayscale pixel-values of those white nodes are lower than the chosen threshold value. By using a simple linear interpolation, we move these white nodes in the direction of the surface boundary toward the locations where the grayscale pixel-value would exactly match the threshold value. There are multiple methods available to move the nodes by linear interpolation. It is important to note that in some cases this linear interpolation might even move the node inside the object.

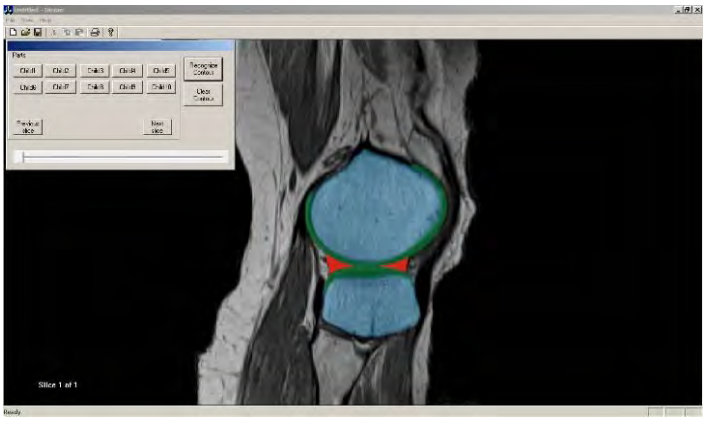

Fig. 4. Segmentation of the knee model from MRI slices. Sagittal view MRI of the left knee. The bone geometry, cartilages and meniscuses are digitized for 3D finite element model

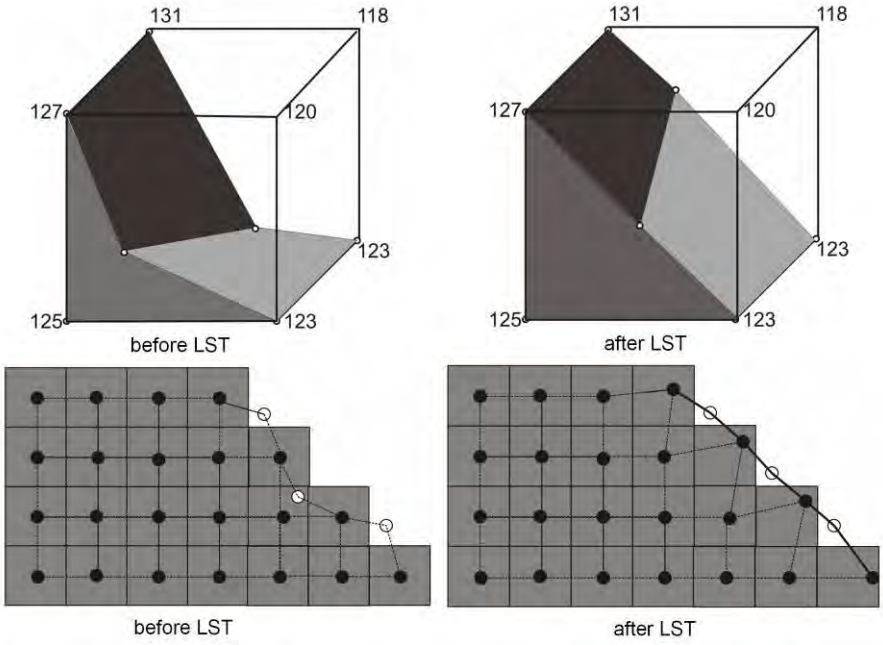

Fig. 5 Grid-Based Hexahedral Algorithm. 3D thresholded voxels (upper panel), and 2D representation of thresholded voxels (bottom panel). The grayscale values are kept in the map of voxel. Laplacian Smoothing Technique (LST). 3D and 2D before LFT (left panel), 3D and 2D after LFT (right panel)

The translation of the nodes may in some cases lead to a distorted (concave) FE-surface. The distortion of the FE-nodes can be evaluated with their Jacobian value. The Jacobian value is a matrix of the derivation of

global to local finite element interpolation function and the quality of any mesh can be directly evaluated by its Jacobian value. Distorted FEs, which are not suitable for subsequent numerical calculations, show a negative Jacobian. To optimize the Jacobian, we implemented the standard Laplacian Smoothing Technique (LST) [16]. The LST usually takes a few loops (repetitions of step ii) over all FEs to achieve positive Jacobian values for all FEs. The results of applying the LST for 3D and 2D cases are shown respectively in the right panels of Fig. 5 ("After LST") [17].

The finite element mesh is presented in Figure 6. Very fine mesh up to one million of finite elements is used.

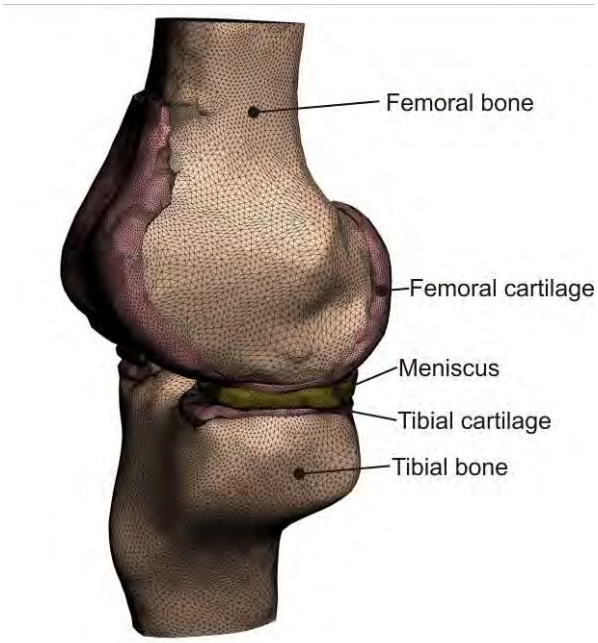

Fig 6. Finite element mesh for different knee segments

Some C pseudo code for contour recognition and 3d reconstruction code are given below. Detailed source is given in the Appendix.

```
void function mesh_generation
for (i = 1; i<=Num_voxel; i++) {
        set voxel=black;
if i is outside object
        set voxel=White;
}
void function surface_generation
for (i = 1; i<=Num_voxel; i++) {
        set Jacobian;
if Jacobian < 0
```

```
        use Lapacian_smoothing_algorithm;
}
void function Laplacian_ smoothing_algorithm
        set Node(x,y,z)
for (i = 1; i<=Num_node_el; i++) {
        X=Sum X(i);
        Y=Sum Y(i);
        Z=Sum Z(i);
        Node(x)=X/ Num_node_el;
        Node(y)=Y/ Num_node_el;
        Node(z)=Z/ Num_node_el;
}
```

For modeling of the cartilage and meniscus we implemented finite element formulation where the nodal variables are: displacements of solid, **U**; fluid pressure, **P**; Darcy's velocity, **Q;** and electrical potential, $\mathbf{\Phi}$. A standard procedure of integration over the element volume is performed and the Gauss theorem is employed. An implicit time integration scheme is implemented, hence the condition that the balance equations are satisfied at the end of each time step is imposed. The system of differential equations for each finite element is:

$$\begin{bmatrix} \mathbf{M}_{uu} & 0 & 0 & 0 \\ 0 & 0 & 0 & 0 \\ \mathbf{M}_{qu} & 0 & 0 & 0 \\ 0 & 0 & 0 & 0 \end{bmatrix} \begin{Bmatrix} {}^{n+1}\ddot{\mathbf{U}} \\ {}^{n+1}\mathbf{P} \\ {}^{n+1}\ddot{\mathbf{Q}} \\ {}^{n+1}\ddot{\mathbf{\Phi}} \end{Bmatrix} + \begin{bmatrix} 0 & 0 & \mathbf{C}_{uq} & 0 \\ \mathbf{C}_{pu} & \mathbf{C}_{pp} & 0 & 0 \\ 0 & 0 & \mathbf{C}_{qq} & 0 \\ 0 & 0 & 0 & 0 \end{bmatrix} \begin{Bmatrix} {}^{n+1}\dot{\mathbf{U}} \\ {}^{n+1}\dot{\mathbf{P}} \\ {}^{n+1}\dot{\mathbf{Q}} \\ {}^{n+1}\dot{\mathbf{\Phi}} \end{Bmatrix}$$
$$+ \begin{bmatrix} \mathbf{K}_{uu} & \mathbf{K}_{up} & 0 & 0 \\ 0 & 0 & \mathbf{K}_{pq} & 0 \\ 0 & \mathbf{K}_{qp} & \mathbf{K}_{qq} & \mathbf{K}_{q\phi} \\ 0 & \mathbf{k}_{\phi p} & 0 & \mathbf{k}_{\phi\phi} \end{bmatrix} \begin{Bmatrix} \Delta\mathbf{U} \\ \Delta\mathbf{P} \\ \Delta\mathbf{Q} \\ \Delta\mathbf{\Phi} \end{Bmatrix} = \begin{Bmatrix} {}^{n+1}\mathbf{F}_u \\ {}^{n+1}\mathbf{F}_p \\ {}^{n+1}\mathbf{F}_q \\ {}^{n+1}\mathbf{F}_\phi \end{Bmatrix} \quad (\mathbf{4})$$

The matrices and vectors are:

$$\mathbf{K}_{q\phi} = -k_{11}^{-1}k_{12}\int_V \mathbf{N}_q^T\mathbf{N}_{\phi,x}dV \quad \mathbf{K}_{\phi q} = k_{21}\int_V \mathbf{N}_{\phi,x}^T\mathbf{N}_{q,x}dV$$
$$\mathbf{K}_{\phi\phi} = -k_{22}\int_V \mathbf{N}_{\phi,x}^T\mathbf{N}_{\phi,x}dV$$
$${}^{n+1}\mathbf{F}_q = \int_V \mathbf{N}_q^T\rho_f\,{}^{n+1}\mathbf{b}dV - \mathbf{K}_{qp}\,{}^{n}\mathbf{P} - \mathbf{K}_{qq}\,{}^{n}\mathbf{Q} - \mathbf{K}_{q\phi}\,{}^{n}\mathbf{\Phi} \quad (\mathbf{5})$$
$${}^{n+1}\mathbf{F}_\phi = \int_A \mathbf{N}_\phi^T\mathbf{n}^T\mathbf{j}\,dA - \mathbf{K}_{\phi p}\,{}^{n}\mathbf{P} - \mathbf{K}_{\phi\phi}\,{}^{n}\mathbf{\Phi}$$

Details about all variables in eqs (4) and (5) are given in [18]. The above equations are further assembled and the resulting FE system of equations is

integrated incrementally, with time step Δt, transforming this system into a system of algebraic equations. A Newmark integration method is implemented for the time integration.

4. Computational modeling results

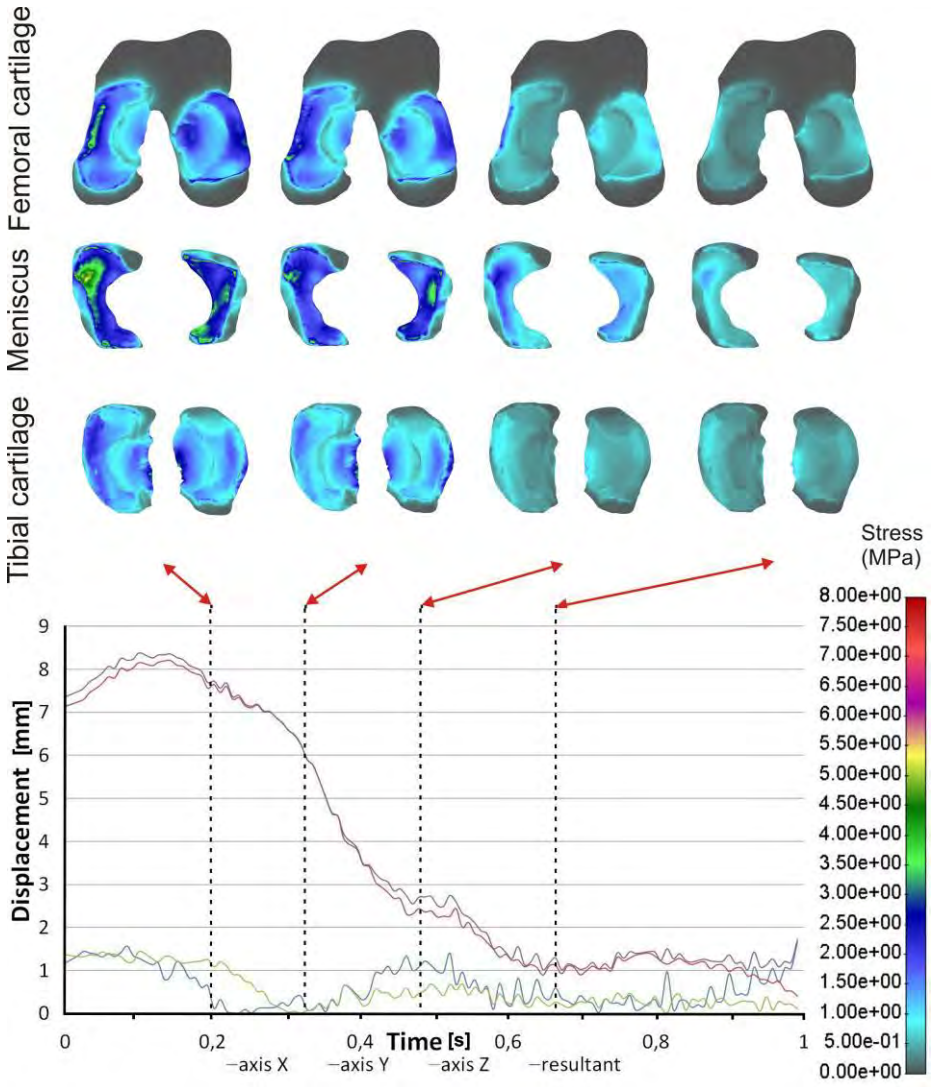

Fig. 7a. Effective von Mises stress distribution for patient specific femoral cartilage, meniscus and tibial cartilage during one gate cycle before surgery

The effective von Mises stress distribution for patient specific plane at femoral cartilage, meniscus and tibial cartilage during one gate cycle is presented in Fig. 7. It can be seen that during 30% of the gait cycle the maximum effective stress up to 8 MPa occurred and the majority of the load occurred on the meniscus part. Higher deformation of the tibia after the surgery induced higher stress on the tibial cartilage part. We presented the effective stress results for the case before (Fig 7a) and after (Fig 7b) the surgery. There is a prolonged higher stress during time cycle after surgery than before surgery.

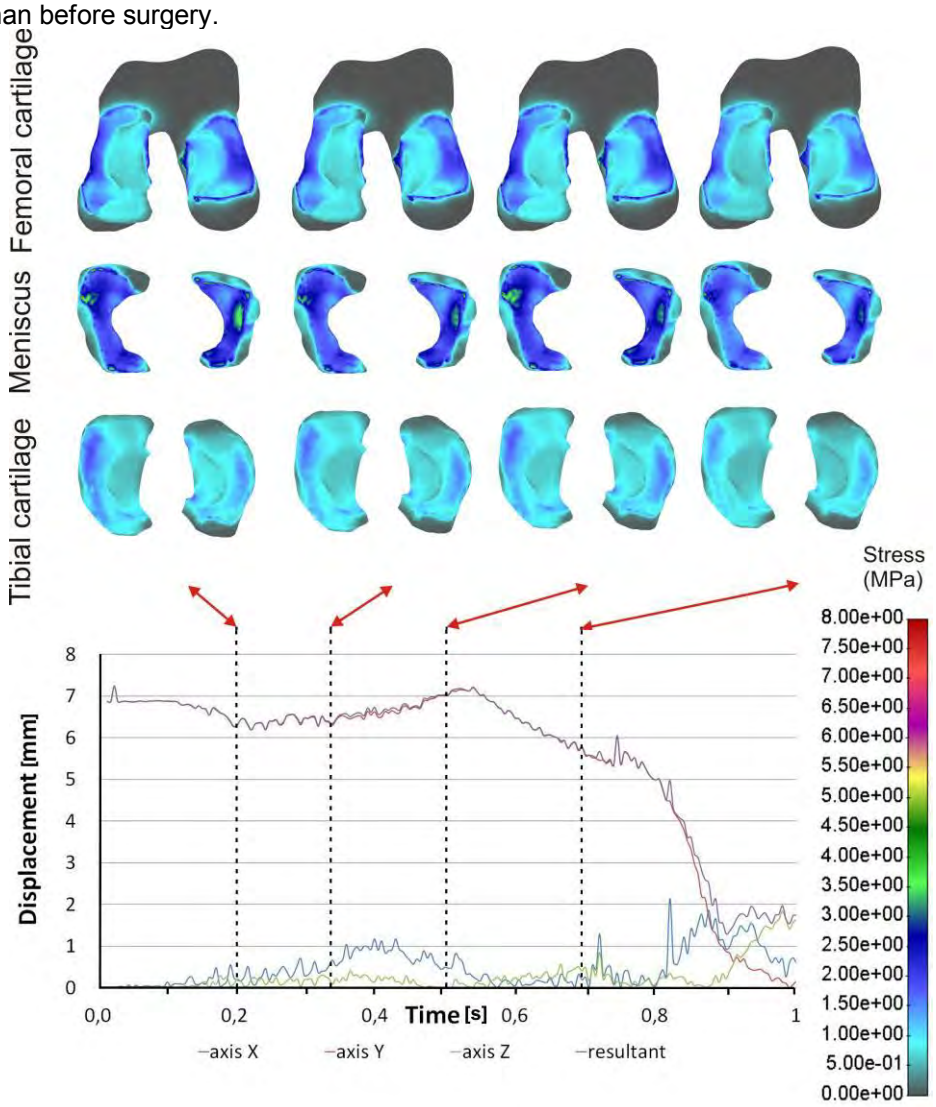

Fig. 7b. Effective von Mises stress distribution for patient specific femoral cartilage, meniscus and tibial cartilage during one gate cycle after surgery

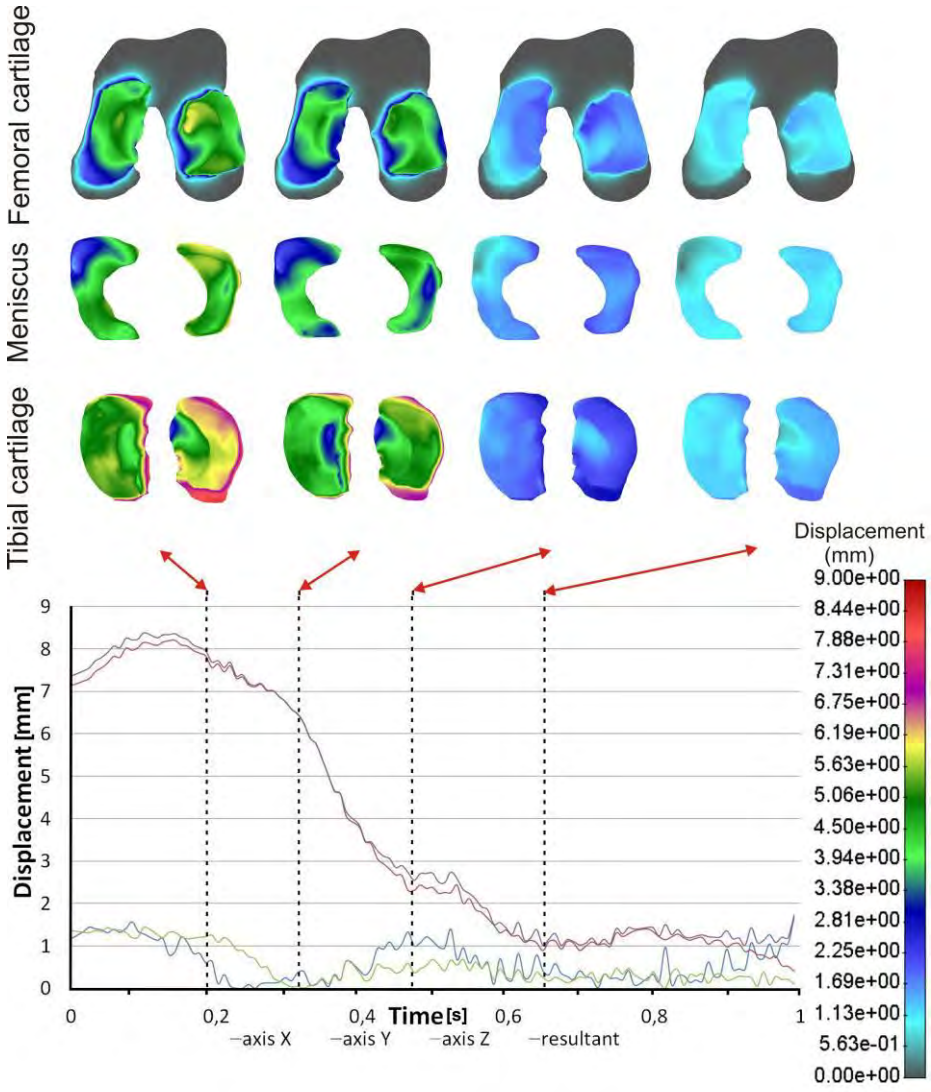

Fig. 8. Displacement distribution for patient specific femoral cartilage, meniscus and tibial cartilage during one gate cycle before surgery

The displacement distribution for patient specific femoral cartilage, meniscus and tibial cartilage during one gate cycle is presented in Fig. 8. Again it is clear that surgical intervention of ACL reconstruction establish the larger range of motion for the knee which is more stable during gate cycle analysis.

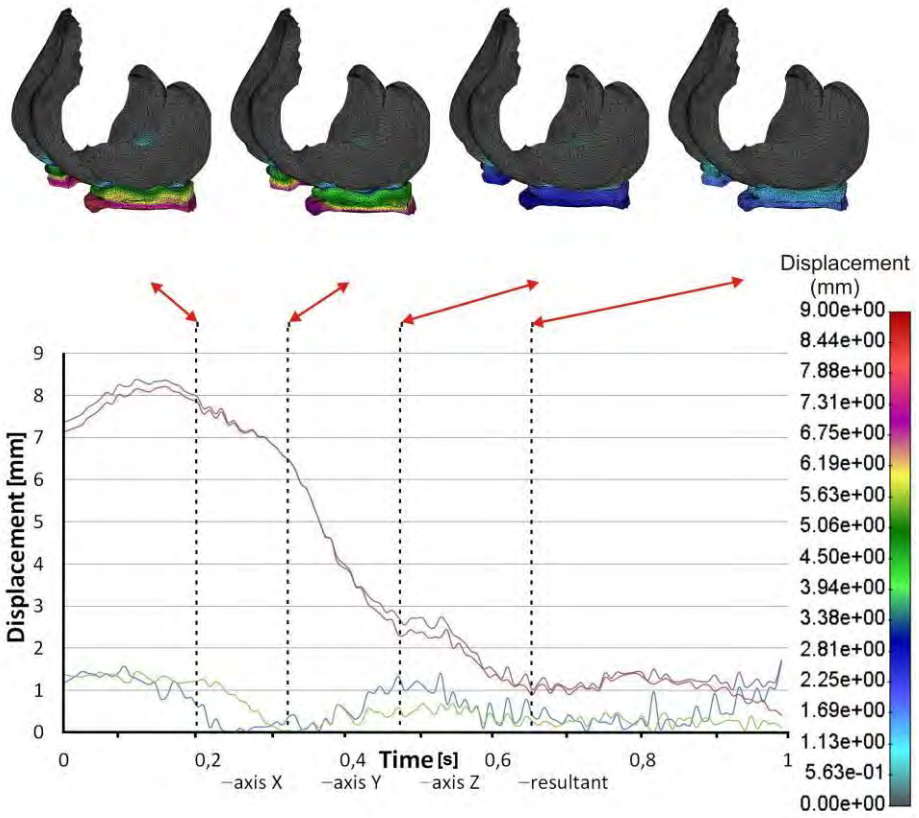

Fig. 9. Displacement distribution in the three-dimensional patient specific FE model during one gate cycle before surgery

Displacement distribution in the three-dimensional patient specific FE model during one gate cycle is presented in Fig. 9. Only femoral cartilage, meniscus and tibial cartilage are presented due to clarify. Obviously large deformation occurred in the tibial cartilage part.

Damage can occur to the tibial cartilage as an isolated condition, or in conjunction with other knee injuries. ACL injuries are commonly associated with damage to the medial and lateral surfaces of the femur and tibia. Other injuries that can lead to articular cartilage damage are those resulting from a forceful impact on the knee joint, such as a tackle in football or soccer. Injury to the articular cartilage will lead to inflammation and pain in the knee joint and in the long term it is known to accelerate the onset of osteoarthritis.

5. Discussion and conclusions

Various interventions and surgical procedures are performed for preventing knee injury. Still there is a lack of fundamental understanding of the biomechanical factors that contribute to the development and progression of knee diseases.

This study offers an innovative and robust approach to assess 3D kinetics of knee and the stress and strain distributions in the knee-based subject-specific biomechanical models of the human knee joint, MRI imaging and measured kinematic data. It could open new avenues for objective assessment of knee functioning pre and post-operation. Some details of algorithms and source code about contour recognition and 3D reconstruction are also given in this paper.

Using kinematic data measured from gait analysis we prescribe displacement on the characteristics marker position and stress and strain distributions were analyzed. It was observed that the maximum effective von Mises stress distribution up to 8 MPa was happen during 30% of the gait cycle. The location of the maximum stress occurred on the meniscus part. Increased deformation of the tibia after the surgery induced higher stress on the tibial cartilage part.

Main contribution of this study is noninvasive effective stress calculation for a specific given patient. Input data are provided from gait analysis experimental measurements and effective stress analysis is calculated from finite element analysis. This will open a new avenue for preoperative and postoperative surgical planning and treatment of the knee for specific patients.

There are also some limitations of the current study. We used material properties from literature data and it will be in future based on advanced image method for moving of the segments during MRI procedure. However, this study shows the ability of the current model to investigate the effect of different biomechanical factors on the stress at the knee joint.

Acknowledgments. This work has been partly supported by Ministry of Education and Science of Serbia, Grants No. III-41007, OI-174028 and project supported by Faculty of Medicine Kragujevac, Grant JP 20/10.

References

1. Fernandez J.W. and Pandy M. G.: Integrating modelling and experiments to assess dynamic musculoskeletal function in humans. Exp Physiol, Vol.91, No. 2, 371–382. (2006)
2. Li G, Lopez O, Rubash H.: Variability of a three dimensional finite element model constructed using magnetic resonance images of a knee for joint contact stress analysis. J Biomed Eng. Vol. 123, 341–346. (2001)

3. Li G, Suggs J, Gill T.: The effect of anterior cruciate ligament injury on knee joint function under a simulated muscle load: a three-dimensional computational simulation. Ann Biomed Eng, Vol. 30, 713–720. (2002)
4. Andriacchi TP, Briant PL, Bevill SL, Koo S.: Rotational changes at the knee after ACL injury cause cartilage thinning. Clin Orthop Relat Res, Vol. 442, 39–44. (2006)
5. Bachrach NM, Valhmu WB, Stazzone E, Ratcliffe A, Lai WM, Mow VC.: Changes in proteoglycan synthesis of chondrocytes in articular cartilage are associated with the time dependent changes in their mechanical environment. J Biomech, Vol. 28, 1561–1569. (1995)
6. Shelburne KB, Pandy MG & Torry M.: Comparison of shear forces and ligament loading in the healthy and ACL-deficient knee during gait. J Biomech, Vol. 37, 313–319. (2004)
7. Yao J, Snibbe J, Maloney M, Lerner AL.: Stresses and strains in the medial meniscus of an acl deficient knee under anterior loading: a finite element analysis with image-based experimental validation. J Biomech Eng. Vol. 128, 135–141. (2006)
8. Yang N.H., Canavan P.K., Nayeb-Hashemi H., Najafi C., Vaziri A.: Protocol for constructing subject - specific biomechanical models of knee joint. Computer Methods in Biomechanics and Biomedical Engineering, Vol. 13, 589 - 603. (2010)
9. Matić A., Ristić B., Devedžić G., Filipović N., Petrović S., Mijailović N., Ćuković S.: Gait analysis in patients with chronic anterior cruciate ligament injury, Serbian Journal of Experimental and Clinical Research, Vol.13, No. 2, 49 - 54. (2012)
10. Brandsson S., Karlsson J., Swärd L., Kartus J., Eriksson B.I., Kärrholm J: Kinematics and Laxity of the Knee Joint After Anterior Cruciate Ligament Reconstruction. The American Journal of Sports Medicine, Vol. 30, 361 – 367. (2002)
11. Isaac D.I., Beard D.J., Price A.J., Rees J., Murray D.W., Dodd C.A.F.: In-vivo sagittal plane knee kinematics: ACL intact, deficient and reconstruction knees. The Knee, Vol. 12, 25 - 31. (2005)
12. Manal K., McClay Davis I., Galinat B., Stanhope S: The accuracy of estimating proximal tibial translation during natural cadence walking: bone vs. skin mounted targets. Clinical Biomechanics Vol. 18, 126 – 131. (2003)
13. Gao B., Cordova M.L., Zheng N.N.: Three-dimensional joint kinematics of ACL-deficient and ACL-reconstructed knees during stair ascent and descent. Human Movement Science, Vol. 31, 222 -235. (2012)
14. Kvist J.: Tibial translation in exercises used early in rehabilitation after anterior cruciate ligament reconstruction Excercises to achieve weight-bearing. The Knee, Vol. 13, 460 - 463. (2006)
15. Scanlan S.F., Chaudhari A.M.W., Dyrby C.O., Andriacchi T.P.: Differences in tibial rotation during walking in ACL reconstructed and healthy contralateral knees. Journal of Biomechanics, Vol. 42, 1817 – 1822. (2010)
16. Freitag L, Plassmann P.: Local optimization based simplicial mesh untangling and improvement. Intl. J. Num. Method. in Engr., Vol. 49, 109-125. (2000)
17. Tsuda, A., Filipovic, N., Haberthür, D., Dickie, R., Matsui, Y., Stampanoni, M. and Schittny, J.C.: Finite element 3D reconstruction of the pulmonary acinus imaged by synchrotron X-ray tomography. J Appl Physiol, Vol. 105, 964-976. (2008)
18. Filipovic N., Basics of Bioengineering. Monograph in Serbian. (2012)

Appendix:

```
void CContourRecognizer::LoadPng(const char *pName)
{
	WCHAR wbuf[512];
	mbstowcs(wbuf, pName, sizeof(wbuf)/sizeof(wbuf[0]));
	Bitmap bmp(wbuf);
	int w = bmp.GetWidth();
	int h = bmp.GetHeight();
	m_Pixmap.InitDim(w, h);
	for(int x=0;x<w;x++)
	{
		for(int y=0;y<h;y++)
		{
			Color cl;
			bmp.GetPixel(x,h-y-1,&cl);
			double tr = cl.GetR()/255.0;
			//if (tr > 0.9) tr = 0;
			m_Pixmap.SetAt(x,y, tr);
		}
	}
}

void CContourRecognizer::LoadDicomFile(const char *pName)
{
	m_Pixmap.Kill();
	CDCMFile dcm;
	dcm.Read(pName);
	int w = dcm.m_nWidth;
	int h = dcm.m_nHeight;
	m_Pixmap.InitDim(w, h);
	for(int x=0;x<w;x++)
	{
		for(int y=0;y<h;y++)
		{
			m_Pixmap.SetAt(x,y, dcm.GetPixelValueD(x,h-y-1));
		}
	}
}

bool CContourRecognizer::Mesh_Generation(const Math3d::M2d &InnerPoint, const Math3d::M2d &OutterPoint)
{
	const int pixCount = 2048;
	const double dInvStep = 1.0 / (double)pixCount;
	double pixValues[pixCount];
	for(int i=0;i<pixCount;i++)
```

```
        {
                double t = i * dInvStep;
                Math3d::M2d cur = InnerPoint * (1-t) + OutterPoint * t;
                pixValues[i] = m_Pixmap.GetLinearWSlopesAt(cur.x, cur.y);
        }
        double tMid;
        for(i=1;i<pixCount;i++)
        {
                double d0 = pixValues[i-1];
                double d1 = pixValues[i];
                if ((d0-m_dLevel)*(d1-m_dLevel) <= 0)
                {
                        tMid = (i-0.5)*dInvStep;
                        break;
                }
        }
        if (i == pixCount) return false;
        return FindIsoPoints(InnerPoint * (1-tMid) + OutterPoint * tMid);
  }

  bool CContourRecognizer::Surface_Generation(const Math3d::M2d
&firstPoint)
  {
        m_IsoPoints.RemoveAll();
        m_IsoPoints.SetSize(0,2000);
        double dLevel = m_Pixmap.GetLinearWSlopesAt(firstPoint.x,
firstPoint.y);
        Math3d::M2d curPoint = firstPoint;
        double curLevel = dLevel;
        Math3d::M2d grad;
        double dStep = m_dStep;
        double dStepSqr = dStep*dStep*1.01;
        int nMaxPts = 3000;
        for(int i=0;i<nMaxPts;i++)
        {
                grad.x = m_Pixmap.GetLinearDifX(curPoint.x, curPoint.y,
0.001);
                grad.y = m_Pixmap.GetLinearDifY(curPoint.x, curPoint.y,
0.001);
                Math3d::M2d moveVec = grad;
                moveVec.Rotate90();
                moveVec.Normalize();
                curPoint += moveVec * dStep;
                for(int c=0;c<3;c++)
                {
                        grad.x = m_Pixmap.GetLinearDifX(curPoint.x,
curPoint.y, 0.0001);
```

```
                        grad.y = m_Pixmap.GetLinearDifY(curPoint.x,
curPoint.y, 0.0001);
                        curLevel =
m_Pixmap.GetLinearWSlopesAt(curPoint.x, curPoint.y);
                        Math3d::M2d corr = grad * ((dLevel - curLevel) /
grad.NormSqr());
                        curPoint += corr;
                }
                m_IsoPoints.Add(curPoint);
                if (m_IsoPoints.GetSize() > 5)
                {
                        if ((curPoint-firstPoint).NormSqr() <= dStepSqr)
break;
                }
        }
        if (i == nMaxPts) ::AfxMessageBox("Can not close contour");
        return (i != nMaxPts);
  }
```

Nenad Filipović received the Ph.D. in bioengineering from the University of Kragujevac, Serbia in 1999. He was Research Associate at Harvard School of Public Health in Boston, USA. He is currently a Professor in Bioengineering at Faculty of Mechanical Engineering, University of Kragujevac, Serbia. His research interests are in the area of fluid mechanics, coupled problems; fluid-structure interaction, heat transfer; biofluid mechanics; biomechanics, multi-scale modeling, discrete modeling, molecular dynamics, computational chemistry and bioprocess modeling. He is author and co-author 6 textbooks and 1 monograph on English language, over 50 publications in peer review journals and over 5 software for modeling with finite element method and discrete methods from fluid mechanics and multiphysics. He leads a number of national and international projects in area of bioengineering.

Velibor Isailović has PhD in area of bioengineering at Metropoliten University, Serbia. His main research interests include coupled problem, fluid-structure interaction, particle methods, finite element methods. He has authored/co-authored more than 8 papers in peer-review journals.

Dalibor Nikolić is PhD student at Faculty of Engineering in University of Kragujevac. His research interests include computer graphics, medical imaging reconstruction, finite element methods and software engineering. He is main research software engineer at Center for Bioengineering at Faculty of Engineering.

Aleksandar Peulić received the Diploma degree in electronic engineering from Faculty of Electronic Engineering, University of Nis, Nis, Serbia, in 1994, the Master of Science in electrical engineering from Faculty of Electronic Engineering, University of Nis, Nis, Serbia, in 2000 and the Ph.D. degree in electrical engineering from the University of Kragujevac, Serbia, in 2007. From avg. 2008 to feb. 2009, he had a postdoctoral education at the University of Alabama in Huntsville. His research interests include microcontrollers systems, wearable sensors and bioengineering. He is Assistant Professor at Technical faculty, University of Kragujevac.

Nikola Mijailović is PhD Student at Faculty of Engineering in University of Kragujevac. His research interests include electronic and hardware development for bioengineering devices and systems. He has also interest in medical imaging and neural network.

Suzana Petrović is R&T assistant at Faculty of Engineering, University of Kragujevac, Serbia. Her major research interests are bioengineering, gait analysis, machine learning, statistics and advanced product and process development. She is coauthor of one book on 3D product modeling and coauthor of chapter in book on CAD/CAM technology. She is also the author or co-author of more than 10 papers in international and national journals or papers presented at international and national conferences.

Saša Cuković is teaching and research assistant and PhD candidate at Faculty of Engineering, University of Kragujevac, Serbia. He was scholarship holder of Ministry of Education, Science and Technological Development of Republic of Serbia and DAAD grant holder at Technical University of Munich. His main research interests include CAD/CAMsystems, reverse engineering and noninvasive 3D reconstruction and modeling in engineering and medicine, augmented reality and computer vision. He has authored/co-authored more than 20 papers.

Radun Vulović is PhD student at Faculty of Engineering in University of Kragujevac. His research interests include sports biomechanics, computer graphicsfinite element methods and software engineering. He is research software engineer at Center for Bioengineering at Faculty of Engineering.

Aleksandar Matić is othopaedic surgeon at Clinical Center Kragujevac, and T&R assistant at the Faculty of Medical Sciences at University Kragujevac (Serbia). His main research interests involve sports injuries and gait analysis. He has authored/coauthored more than 30 research papers, published in national journals or presented at international and national conferences.

Nebojša Zdravković received the Ph.D. in bioengineering from the University of Kragujevac, Serbia in 2000. He is currently a Associate Professor in Informatics and Medical Statistics at Faculty of Medical Science, University of Kragujevac, Serbia His research interests are in data mining,

statistical methods, finite element method fluid mechanics, coupled problems.

Goran Devedžić is Professor at Faculty of Engineering, University of Kragujevac, Serbia. His research interests focus on the advanced product and process development, industrial and medical application of soft computing techniques, and bioengineering. He has authored/co-authored more than 100 research papers, published in international and national journals or presented at international and national conferences, as well as three books on CAD/CAM technology and 3D product modeling.

Branko Ristić is Associate Professor at Faculty of Medical Sciences, University of Kragujevac, Serbia. His research interests include hip and knee arthroplasty and bioengineering of musculo-skeletal system. He is the author/co-author of more than 100 research papers, six chapters in books of orthopedics and bioengineering. He was actively involved in several research projects addressing bioengineering and total hip and total knee arthroplasty. Currently he is a Head of Clinic for Orthopedics and Traumatology at Clinical Center Kragujevac, Serbia, and the President of the Regional Medical Chamber for Central and Western Serbia.

Received: May 31, 2012; Accepted: December 31, 2012.